
Article:
Burchill, Laura, Males, Alexandra orcid.org/0000-0002-7250-8300, Kaur, Arashdeep et al. (2 more authors) (2023) Structure, function and mechanism of N-glycan processing enzymes:endo-α-1,2-mannanase and endo-α-1,2-mannosidase. Israel Journal of Chemistry. e202200067. ISSN 0021-2148

https://doi.org/10.1002/ijch.202200067

Review

Israel Journal of Chemistry
www.ijc.wiley-vch.de

doi.org/10.1002/ijch.202200067

Structure, Function and Mechanism of N-Glycan Processing Enzymes: *endo*-α-1,2-Mannanase and *endo*-α-1,2-Mannosidase

Laura Burchill,[a] Alexandra Males,[b] Arashdeep Kaur,[a] Gideon J. Davies,[b] and Spencer J. Williams*[a]

Abstract: While most glycosidases that act on N-linked glycans remove a single sugar residue at a time, *endo*-α-1,2-mannosidases and *endo*-α-1,2-mannanases of glycoside hydrolase family GH99 cut within a chain and remove two or more sugar residues. They are stereochemically retaining enzymes that use an enzymatic mechanism involving an epoxide intermediate. Human *endo*-α-1,2-mannosidase (MANEA) trims glucosylated mannose residues; the endo-mannosidase pathway provides a glucosidase-independent pathway for glycoprotein maturation. Cell-active MANEA inhibitors alter N-glycan processing and reduce infectivity of dengue virus, demonstrating that MANEA has potential as a host-directed antiviral target. Sequence-related enzymes from gut *Bacteroides* spp. exhibit *endo*-α-1,2-mannosidase activity and are a fruitful test bed for structure-guided inhibitor development. The genes encoding the *Bacteroides* spp. enzymes sit within polysaccharide utilization loci and are preferential *endo*-α-1,2-mannanases.

Keywords: carbohydrates · glycoproteins · endomannosidase pathway · glycosidase · iminosugar

1. Introduction

It is estimated one quarter to one half of eukaryotic proteins are glycoproteins that carry N-linked glycans.[1–2] N-linked glycans are diverse and complex carbohydrate structures attached through a core chitobiose residue to asparagine.[3] N-linked glycosylation is a common protein modification within eukaryotes and plays a critical role in folding, quality control and trafficking of newly synthesized glycoproteins,[1,4] and in the structure and function of the mature glycoproteins.[5–6] Because of the central role of N-linked glycans, there is keen interest in the development of inhibitors both as cell biology reagents to facilitate the study of the pathway and proteins dependent upon it, as well as to control the function of N-linked glycoproteins.

N-linked glycosylation is initiated within the endoplasmic reticulum. The first step is catalyzed by oligosaccharyltransferase, which transfers a preformed triglucosylated mannosyl-chitobiose linked to dolichol pyrophosphate ($Glc_3Man_9GlcNAc_2$–PP–Dol) to nascent polypeptides, containing an Asn–Xxx–Ser/Thr consensus sequence, while still attached to ribosomes (Figure 1).[7–8] Immediately after transfer of the glycan, trimming of sugar residues takes place to facilitate the folding, trafficking and quality control of newly synthesized N-linked glycoproteins in both the ER and Golgi apparatus.[1] Within the ER, key steps in this pathway include the trimming of glucose residues by α-*exo*-glucosidases I and II, which allow monoglucosylated glycoproteins to engage with the calnexin/calreticulin folding lectins, the release of correctly folded deglucosylated glycoproteins and their transport to the Golgi apparatus. Quality control of folding is achieved by the glucosyltransferase UGGT1, which acts as a folding sensor by reglucosylating unfolded proteins, and allowing them to reengage with calnexin/calreticulin and additional attempts at folding.[9] Folding incompetent and misfolded N-glycoproteins are degraded through the ER-associated degradation pathway (ERAD), which involves recognition of glycoproteins with delayed exit from the ER through the slow degradation of the B and C mannose branches through the action of the EDEM α-mannosidases,[10] their retrotranslocation to the cytosol, ubiquitinylation and proteasomal degradation.[11]

Subject to some minor variations, the classical N-linked glycan processing pathway within the ER is broadly conserved from yeast to humans.[12] However, in many animals including humans, there is an alternative, α-glucosidase independent route for deglucosylation of glycoproteins enabled by a unique, endo-acting enzyme termed *endo*-α-1,2-mannosidase (MANEA; EC 3.2.1.130).[13] MANEA emerged late in evolution and its distribution is largely limited to members of

[a] *L. Burchill, A. Kaur, S. J. Williams*
School of Chemistry and Bio21 Molecular Science and Biotechnology Institute, University of Melbourne, Parkville, Victoria, Australia 3010
E-mail: sjwill@unimelb.edu.au
[b] *A. Males, G. J. Davies*
Department of Chemistry, University of York, York YO10 5DD, United Kingdom

the phylum Chordata (placental and marsupial mammals, birds, reptiles, amphibians, and fish).[14] MANEA cleaves the glucosylated mannose from the A-branch of N-linked glycans such as $Glc_{1-3}Man_9GlcNAc_2$ (and variants trimmed in the B and C branches), releasing $Glc_{1-3}Man$ oligosaccharides and $Man_8GlcNAc_2$. MANEA is primarily active within the Golgi apparatus[15–16] allowing deglucosylation and further processing of ER-escaped glucosylated high mannose N-linked glycoproteins.[16] This may include those that fold independently of the calnexin/calreticulin system; MANEA also cleaves unfolded glycoproteins.[17] Evidence for the importance of the *endo*-α-1,2-mannosidase pathway for glycoprotein maturation is provided by individuals with a congenital disorder of glycosylation (CDG) in which glucosidase I (MOGS) activity is deficient. MANEA activity is sufficient to partially rescue glycoprotein synthesis and this explains the excretion of Glc_3Man tetrasaccharide in their urine.[18] Under normal conditions MANEA plays an important role in flux through the N-glycosylation pathway.[19] In the event of inhibitor blockade of glucosidase I/II activity (such as with deoxynojirimycin or castanospermine), MANEA can rescue as much as 50% of glycoprotein flux through the Golgi apparatus, depending upon expression levels and cell type.[20–21]

MANEA falls within glycoside hydrolase family 99 (GH99) of the Carbohydrate active enzyme (CAZy) classification (www.cazy.org;[22] www.cazypedia.org[23]).[24] Aside from the eukaryotic GH99 members, this family also contains a range of bacterial homologues including those from human gut bacteria. In 2010, the laboratories of the present authors initiated a collaboration to understand the molecular basis of *endo*-α-1,2-mannosidase function and to develop new inhibitors that could be used to study its function and mechanism. In this review, we will describe preliminary studies that commenced with bacterial model proteins, which have sequences related to human *endo*-α-1,2-mannosidase, that led to demonstration that they have similar function and the first 3D structures of GH99 family members. The bacterial model enzymes proved a test-bed for inhibitor development, leading to extremely potent inhibitors. Moreover, they were an excellent system for mechanistic studies of enzymes in GH family 99 that, ultimately, revealed an unprecedented enzymatic reaction pathway proceeding through a 1,2-anhydro sugar (epoxide) intermediate. Unexpectedly, this work led to the discovery of a new enzyme activity, *endo*-α-1,2-mannanase (EC 3.2.1.198), for gut bacterial enzymes operating on a related N-glycan structure within the fungal cell wall. Finally, returning to human *endo*-α-1,2-mannosidase, we were able to apply lessons learned through studies on the bacterial homolog to solve the 3D structure of this enzyme and develop new inhibitors. These were shown to be effective in cell-based studies and were shown to have potential as host-directed antivirals for enveloped viruses.

Laura Burchill is a postdoctoral research fellow working with Prof. Spencer Williams at the University of Melbourne. Laura graduated with a BSc (Hons) from Monash University in 2016. She completed her PhD at the University of Adelaide with Assoc. Prof. Jonathan George in 2021. Her research interests involves the synthesis of natural products and elucidation of biochemical pathways.

Alexandra Males is a postdoctoral research associate in carbohydrate enzymology working in the group of Prof. Gideon Davies at the York Structural Biology Laboratory, University of York. In 2020, she completed her PhD in Biological Chemistry from the University of York under the guidance of Prof. Gideon Davies. Currently, her research is focused on the enzymatic biosynthesis of sugar polymers and their implications in diseases.

Arashdeep Kaur is a PhD candidate at University of Melbourne. She received her BSc (Hons) in Chemistry from the Guru Nanak Dev University and MSc (Chemical Sciences) from La Trobe University. Her current research in the laboratory of Prof. Spencer Williams is aimed at discovery of degradation pathways for natural products.

Gideon Davies is currently the Royal Society Ken Murray Research Professor at the University of York. His area of work is the structural and chemical biology of carbohydrate-active enzymes and their glycobiology. Gideon received his PhD from the University of Bristol in 1990, and went on to postdoctoral research at EMBL Hamburg and CNRS Grenoble. Gideon was elected a Fellow of The Royal Society and a member of the European Molecular Biology Organization in 2010.

Spencer Williams is Professor of Chemistry at the University of Melbourne. He has interests in carbohydrate processing enzymes and pathways, medicinal chemistry, and glycolipid immunology. Spencer received his PhD from the University of Western Australia (Bob Stick), and undertook postdoctoral research at the University of British Columbia (Withers) and University of California at Berkeley (Bertozzi). He thanks Prof Bertozzi for superb mentoring and an exceptional postdoctoral experience.

Israel Journal of Chemistry

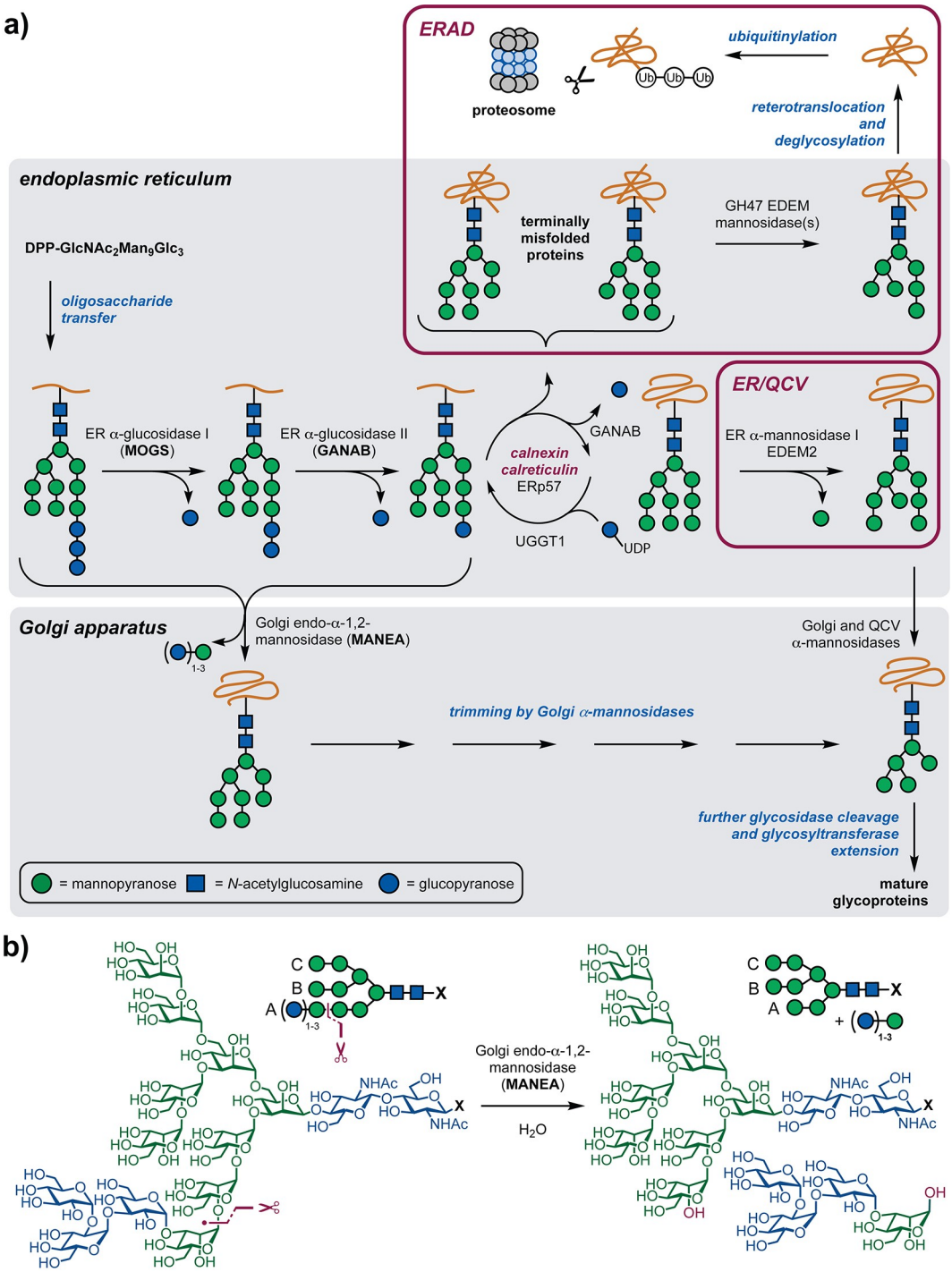

Figure 1. N-linked glycosylation in the secretory pathway. a) classical and endomannosidase pathways. b) Reaction catalyzed by *endo*-α-1,2-mannosidase (MANEA). MANEA cleaves mono-, di- and triglucosylated mannose residues in the A branch of N-linked glycans and free oligosaccharides.

Israel Journal of Chemistry

2. Family GH99 Homologues of Human MANEA from Gut Bacteria are Endo-α-1,2-Mannosidases

The genomes of the human gut bacteria *Bacteroides thetaiotaomicron* and *Bacteroides xylanisolvens* each encode a single GH99 family member (*Bt*GH99 and *Bx*GH99, respectively). Using commercial $GlcMan_9GlcNAc_2$, recombinantly expressed *Bt*GH99 was shown to cleave the glucosylated mannose (on branch A) to produce $Man_8GlcNAc_2$.[25] This observation was in agreement with contemporaneous studies on another bacterial GH99 member, Sama99 from *Shewanella amazonensis*.[26] The activity of *Bt*GH99 was studied using fluorescently-labelled $Glc_3Man_7GlcNAc_2$ and revealed kinetic parameters of $K_M = 83\ \mu M$ and $k_{cat}/K_M = 2.6\ s^{-1}\ mM^{-1}$,[25] data in alignment with the K_M value of 55 μM determined for the rat liver MANEA studied by Lubas and Spiro.[15] Using a highly reactive substrate α-glucosyl-1,3-α-mannosyl fluoride, ^1H NMR analysis revealed that the initial product of enzymatic action was α-glucosyl-1,3-α-mannose and thus that *Bt*GH99 (and by inference all members of family GH99) act with retention of anomeric stereochemistry.[25]

Endo-α-1,2-mannosidase is inhibited by α-glucosyl-1,3-deoxymannojirimycin (GlcDMJ), an iminosugar inhibitor that was developed by Spiro and colleagues by modification of the known exo-α-mannosidase inhibitor deoxymannojirimycin (DMJ) with an *endo*-α-1,2-mannosidase-targeting α-1,3-linked glucosyl residue (Figure 2).[27–28] Inspired by their approach, we designed and synthesized the azasugar α-glucosyl-1,3-isofagomine (GlcIFG) (Figure 2a).[25] Isothermal titration calorimetry (ITC) revealed that *Bt*GH99 binds both GlcDMJ and GlcIFG with K_d values of 24,000 nM and 625 nM, respectively. 3D structures of *Bt*GH99 and *Bx*GH99 were determined by X-ray crystallography (Figures 2b and c) and revealed an $\alpha\beta_8$ barrel fold with a central open cleft formed from extended loop regions. Crystals of *Bt*GH99 proved recalcitrant to complex formation, but crystals of *Bx*GH99 proved highly amenable to formation of complexes, allowing structural

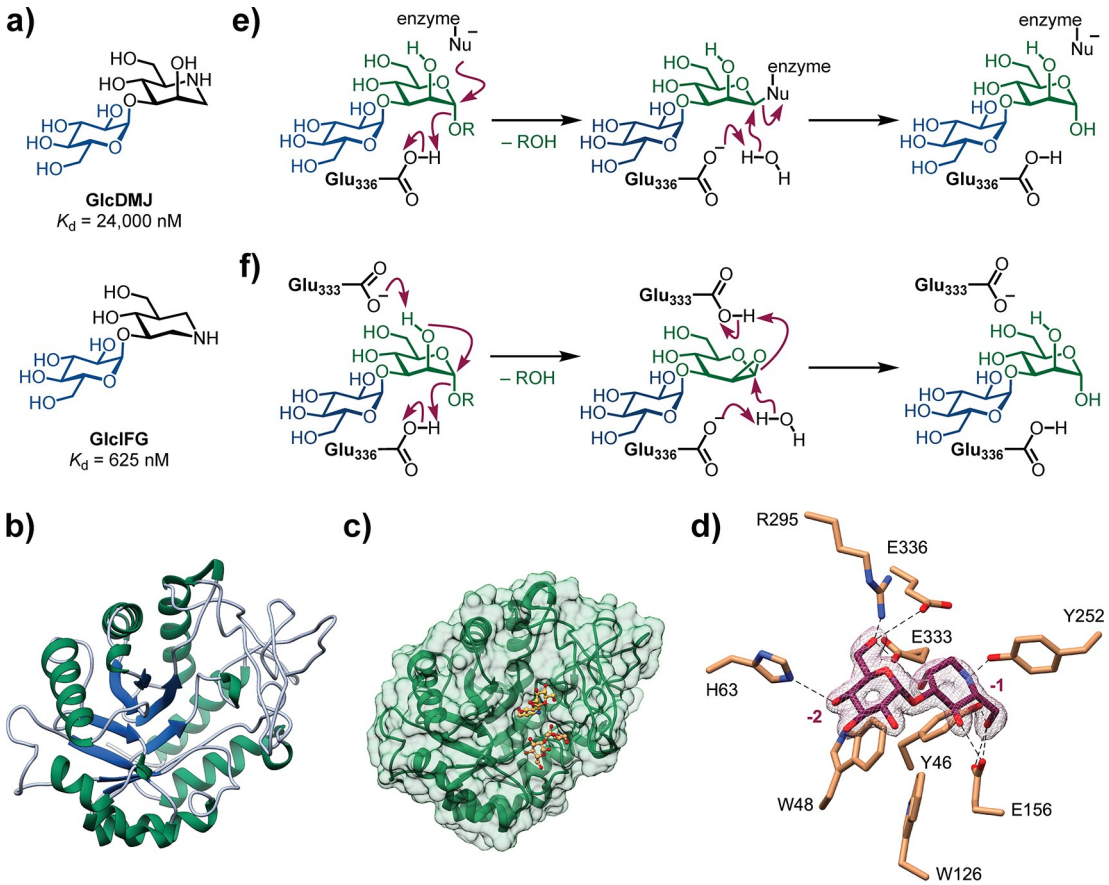

Figure 2. Bacterial family GH99 enzymes are *endo*-α-1,2-mannosidases and provide insight into structure and mechanism in this family. a) Iminosugar (GlcDMJ) and azasugar (GlcIFG) inhibitors of *B. thetaiotaomicron* GH99 (*Bt*GH99). b) 3D structures of apo *Bt*GH99 (PDB 4ACZ) and c) *B. xylanisolvens* GH99 (*Bx*GH99) complex with GlcIFG (yellow) and α-1,2-mannobiose (orange) (PDB 4AD4). d) View of the active site of *Bx*GH99 with residues in orange, and GlcDMJ (purple) (PDB 4AD3). The maximum-likelihood/σ_A-weighted $2F_{obs}–F_{calc}$ map shown in purple is contoured at 0.57 $e^-/Å^3$. e) Proposed classical Koshland two-step retaining mechanism proceeding via a glycosyl-enzyme intermediate. No appropriately situated enzymic nucleophile was evident in the 3D X-ray structure. f) Proposed neighboring group participation mechanism via a 1,2-anhydro sugar (epoxide) intermediate.

determination of binary complexes with GlcDMJ and GlcIFG (Figure 2d), and ternary complexes with each inhibitor and the reducing-end product α-1,2-mannobiose.

The binary and ternary inhibitor complexes revealed the identity and location of the family GH99 active site residues and highlighted a conundrum in that the typical enzymatic nucleophile (Asp, Glu, Tyr or Cys) implicated in a classical retaining hydrolysis mechanism that proceeds through a glycosyl enzyme intermediate was absent.[25] By way of explanation, retaining mannosidases from other GH families operate through a two-step Koshland mechanism with the involvement of two carboxylate residues, one acting as nucleophile and the other as general acid/base (Figure 2e).[29] In the first step, nucleophilic attack at the anomeric carbon by the enzymatic carboxylate forms a glycosyl enzyme intermediate, with the second enzymatic carboxylic acid acting as a general acid to assist in the departure of the aglycon. In the second step, the glycosyl enzyme intermediate is hydrolysed, regenerating the catalytic nucleophile, with general base assistance from the other carboxylate residue. Yet, it was not possible to identify a nucleophilic amino acid located within a feasible distance to perform this role in any of the complexes with sugar-shaped heterocycles. Therefore, we tentatively proposed a neighboring group participation mechanism in which the substrate 2-OH could act as a nucleophile to perform an internal substitution leading to a reactive 1,2-anhydrosugar (epoxide) intermediate, which would be hydrolysed in a second step to give overall retention of anomeric stereochemistry (Figure 2f). While this mechanism was unprecedented in enzymatic catalysis, it had strong precedent in the base-mediated hydrolysis of α-mannosides. However, tempering our enthusiasm, we were aware that glycosidase mechanism involving an epoxide had previously been proposed but disproven for LacZ β-galactosidase.[30–32] Gratifyingly, as will be described below, our speculative suggestion based solely on interpretation of static 3D structures has since been borne out through careful mechanistic investigations.

3. Discovery of Endo-α-1,2-Mannanase Activity of GH99 Enzymes from Human Gut Bacteria

Polysaccharide utilization loci (PUL) are physically linked genes encoding enzymes and associated import machinery that orchestrate the breakdown of complex carbohydrates. Transcriptional analysis of *B. thetaiotaomicron* grown on a yeast mannan source from *Saccharomyces cerevisiae*, revealed activation of three genetic loci (MAN-PUL1/2/3) containing around 50 genes, including many α-mannosidases and α-mannanases.[33] On the other hand, bacterial growth on a mammalian high mannose N-glycan did not lead to activation of these genetic loci, pointing to a specialized function of these PULs in degrading yeast mannan. The gene encoding *Bt*GH99 (BT3862) lies within MAN-PUL3 (Figure 3a). Careful consideration of the structure of *S. cerevisiae* mannan revealed a structural element almost identical to the αGlc-1,3-αMan-1,2-αMan-1,2-αMan structure embedded within the A branch of the mammalian glucosylated high mannose N-glycan ($Glc Man_9 GlcNAc_2$); αMan-1,3-αMan-1,2-αMan-1,2-αMan differs only in the stereochemistry at the terminal sugar residue (Figure 3b). Based on this observation, we synthesized fluorogenic 4-methylumbelliferone (MUF) glycosides, αGlc-1,3-αMan-MUF and αMan-1,3-αMan-MUF (Figure 3c), and showed that the latter was a better substrate for both *Bt*GH99 ($\Delta\Delta G^{\neq} = -4.7\ kJ\,mol^{-1}$) and *Bx*GH99 ($\Delta\Delta G^{\neq} = -6.3\ kJ\,mol^{-1}$).[34] Moreover, *Bt*GH99 turned over αMan-1,3-αMan-1,2-αMan-1,2-αMan to give the corresponding disaccharides.[33–34] Thus, *Bt*GH99 assists the breakdown of complex yeast mannan by removing a limited proportion of the terminal αMan-1,3-αMan disaccharides, exposing the α-1,6-mannan backbone to family GH76 α-1,6-mannanases, which trim the yeast mannan into smaller fragments for import into the cell.

Sequence similarity networks (SSNs) allow visualization of sequence similarity across members of protein families.[35] All-by-all BLAST alignment of family GH99 member sequences and visualization of the results as an SSN reveals that the family can be segregated into several presumably isofunctional clusters (Figure 4). Human and rat MANEA fall into a eukaryotic cluster of sequences that contains *endo*-α-1,2-mannosidases, while the *Bacteroides* spp. *endo*-α-1,2-mannosidases/*endo*-α-1,2-mannanases reside within a distinct cluster of bacterial sequences that also contains the *S. amazonensis endo*-α-1,2-mannosidase Sama99.[26] Interestingly, a distinct cluster of Actinobacteria is evident that contains no characterized members, suggesting the possibility for discovery of new activities within this family.

4. Exploring Inhibitor Design for Bacterial Endo-α-1,2-Mannanases

Given the preference of *Bt*GH99 and *Bx*GH99 for αMan-1,3-αMan configured substrates over αGlc-1,3-αMan, we synthesized ManIFG (Figure 5a).[34] ManIFG bound *Bt*GH99 with $K_{d=}$140 nM (for *Bx*GH99, $K_{d=}$217 nM), approximately 4-fold more tightly than for GlcIFG. The 3D X-ray structure gave insight into the structural basis of this preference, which arises from a hydrophobic interaction of Trp126 with C2 that cannot be achieved in D-*gluco* configured substrates and inhibitors such as GlcIFG. Interestingly, despite the absence of a 2-hydroxyl group in the isofagomine moiety, GlcIFG and ManIFG are much better inhibitors of *Bt*GH99/*Bx*GH99 than the corresponding GlcDNJ (*Bt*GH99, $K_{d=}$24,000 nM). To explore this issue, we synthesized the corresponding noeuromycin[36] analogue, ManNOE, which reinstates the 2-hydroxy group (but at the expense of facile epimerization arising from the hemiaminal group).[37] ManNOE bound *Bt*GH99 with K_d of 30 nM, a 5-fold improvement over ManIFG (for *Bx*GH99, $K_d = 13$ nM, 17-fold improvement over

Israel Journal of Chemistry

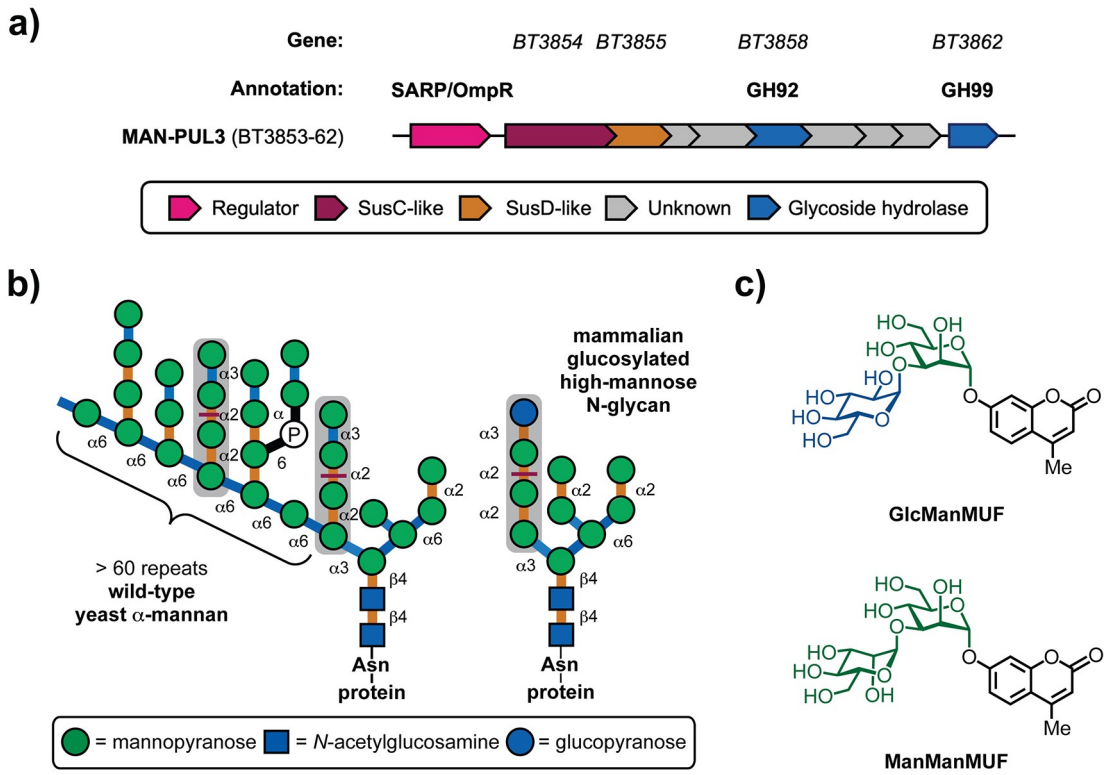

Figure 3. Family GH99 enzymes from *Bacteroides* spp. are *endo*-α-1,2-mannanases. a) Structure of MAN-PUL3, the GH99-containing polysaccharide utilization locus activated by growth on fungal α-mannan. b) Comparison of the structures of yeast mannan from *Saccharomyces cerevisiae* and mammalian $GlcMan_9GlcNAc_2$. c) Fluorogenic substrates used to assess preference for yeast α-mannan and mammalian glucosylated high mannose N-glycans.

ManIFG), highlighting the value of maximizing the resemblance to the substrate (Figure 5a).

Further exploration of inhibitor concepts explored the binding of molecules with sp^2-hybridized anomeric centres that could mimic oxocarbenium ion-like transition states. Building on a report by Spiro and coworkers stating that Glc-glucal was an effective inhibitor of mammalian endomannosidase,[28] we synthesized Man-Glucal (Figure 5c).[37] Glucals are typically slow substrates for classical retaining glycosidases that use an enzymic nucleophile, resulting in the addition of the nucleophile to the enol ether to make a 2-deoxyglycosyl enzyme, which hydrolyses to give a 2-deoxy sugar. Man-Glucal bound *Bt*GH99 with $K_d = 111$ μM (111,000 nM), and the structure of the *Bx*GH99.Man-Glucal complex revealed the glucal ring intact, further evidence for the lack of an enzymatic nucleophile (Figure 5d).

Inspired by the effectiveness of the α-mannosidase inhibitor and transition state analogue mannoimidazole (ManIm),[29] we synthesized ManManIm (Figure 5e).[38] A dissociation constant could not be obtained for ManManIm using isothermal titration calorimetry; nonetheless the structure of the *Bx*GH99. ManManIm complex revealed the ManIm moiety to be in an unusual $^2H_3/E_3$ conformation, which is unusual for an α-mannosidase, but is consistent with mimicry of the proposed transition state conformation (*vide infra*) (Figure 5f).

Although not discussed in depth here, the interested reader is referred to further work on inhibitor design including α-glucosyl-swainsonine (Fleetamine),[39] α-mannosyl-1,3-(1,2-dideoxymannose),[37] the carbasugar GlcChex,[37] α-mannosyl-1,3-(2-amino-1-deoxymannojirimycin) ($Man2NH_2DMJ$),[38] and α-1,3-glucosyl carbasugar-aziridine (Figure 6).[40]

5. An Epoxide Intermediate in Glycosidase Catalysis

To provide more direct evidence in favor of the proposed 1,2-anhydro sugar reaction mechanism of GH99, we employed a combined computational, structural and experimental approach.[41–42] Initially, we obtained structural 'snap-shots' of the proposed species along the reaction coordinate using a variety of ligands (Figure 7). A 3D structure corresponding to a Michaelis complex of an inactive mutant of *Bx*GH99 (E333Q) with the tetrasaccharide αMan-1,3-αMan-1,2-αMan-1,2-αMan-OMe revealed limited substrate distortion in the reactive −1 subsite, with the −1 ring in a $^4C_1$ conformation distorted towards ^2E (Figure 7a).[41–42] A ternary complex of α-1,3-mannobiose and α-1,2-mannobiose gave insight into the ^4E conformation of the product complex (Figure 7c), and together

Israel Journal of Chemistry

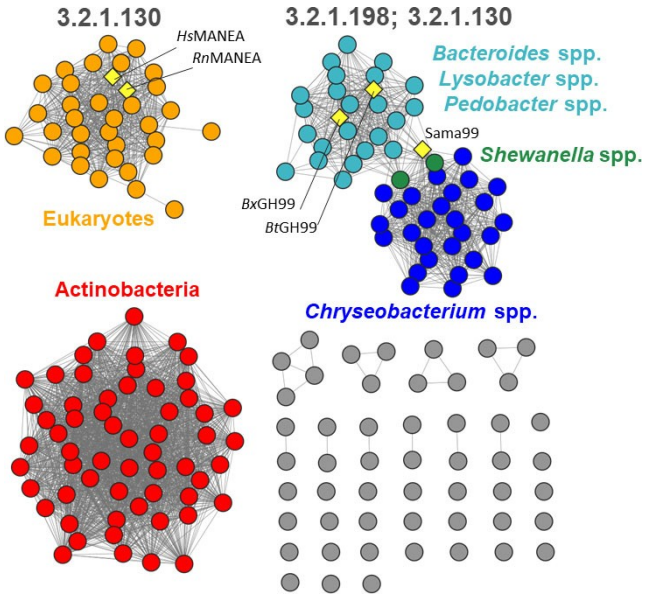

Figure 4. Family GH99 sequence similarity network (SSN). SSN of 200 sequences from the CAZy database with an alignment score threshold of 95. Nodes colored based on taxonomy. Functionally characterised GH99 members are represented as yellow diamond shape and are labelled (UniProt ID: Q5SRI9, Q5GF25, D6D1 V7, Q8A109 and A1S2A2). SSN was generated using the EFI-EFT tool (https://efi.igb.illinois.edu/efi-est/).[60]

these two complexes defined the start and end of the reaction coordinate. Insight into the reaction pathway was obtained using molecular dynamics and QM/MM metadynamics simulations. The 3D structure of the Michaelis complex was used as input, and a wild type Michaelis complex computational model was created, by *in silico* reverting the mutated E333Q residue back to wildtype. The free energy landscape reconstructed from the simulation demonstrated the Michaelis complex in a ^{2}E conformation is transformed to a 1,2-anhydro sugar in a $^{4}E/^{4}H_{5}$ conformation, with an energy barrier of $\Delta G^{\ddagger} = 15$ kcal mol^{-1}. As 1,2-anhydro sugars are highly reactive compounds, we synthesized the more stable cyclohexane epoxide analogue, as well as the corresponding cyclohexane aziridine.[40–41] The cyclohexane epoxide was a slow substrate for *Bt*GH99 and *Bx*GH99, and reacted to give the 1,2-*trans*-diol. However, the aziridine was stable to enzyme action, and this allowed the acquisition of a binary complex with *Bx*GH99 and a ternary complex with α-1,2-mannobiose (Figure 7b). Collectively, the conformation of the −1 ring in the Michaelis, transition state and intermediate complexes is consistent with a $^{2}E/^{2}H_{3} \rightarrow [E_{3}]^{\ddagger} \rightarrow {}^{4}E$ conformational itinerary for GH99 enzymes.

While the above data are consistent with the proposed mechanism involving neighboring group participation by O2, they do not directly demonstrate its involvement. We employed kinetic isotope effects (KIEs) to probe the involvement of O2 in the mechanism. Initially, to measure 'benchmark' KIEs for neighboring group participation we studied the alkaline solvolysis of *p*-nitrophenyl α-D-mannopyranoside (PNPMan),[43] a reaction that is known to proceed by neighboring group participation by a 2-oxyanion via a 1,2-anhydrosugar intermediate.[44] We employed a highly sensitive direct NMR method that involved competition with light and heavy isotopologues each possessing an NMR active nucleus on a site adjacent to the light/heavy isotope.[45] NMR spectroscopy was used to monitor reaction progress for base promoted hydrolysis of PNPMan at the NMR active nucleus and measure competitive KIEs. This provided characteristic KIEs including a strikingly large $^{16}O/^{18}O$ KIE for O2 of 1.044 ± 0.006, $^{12}C/^{13}C$ KIE for C1 of 1.026, and $^{1}H/^{2}H$ KIE for H1 of 1.112 (Figure 7e).[43] A series of five isotopologues of αMan-1,3-αMan-1,2-αMan-1,2-αMan-OMe with appropriate heavy isotope labels introduced into the −1 sugar residue were chemically synthesized and used to measure competitive KIEs for *Bt*GH99. The KIE values reveal the $^{1}H/^{2}H$ KIE for H1 of 1.123, $^{12}C/^{13}C$ KIEs for C1 of 1.030, and $^{16}O/^{18}O$ KIE for O2 of 1.052 (Figure 7d). The carbon-13 KIE of 1.030 is consistent with an S_N2 reaction and exploded associative transition state. The α-secondary deuterium KIE $^{1}H/^{2}H$ KIE for H1 of 1.123 for glycosidic bond fission informs on rehybridization from sp^3 to sp^2 at the transition state but is smaller than for reactions that proceed through bona fide glycopyranosylium ions, consistent with an exploded associative transition state. The $^{16}O/^{18}O$ KIE of 1.052 for O2 is diagnostic for involvement of O2 as a nucleophile at the transition state, and points to a critical role for E333 as a general base in the deprotonation of the 2-hydroxyl of the reactive mannose residue. Collectively, these KIEs for endo-α-1,2-mannanase catalyzed hydrolysis are consistent with those measured for the base-catalyzed hydrolysis of PNPMan.

6. Exploiting the 1,2-Anhydro Sugar Mechanism for Reactive Probes

Activity based protein profiling reagents are useful reactive probes that involve an inhibitor warhead, and a reporter tag such as a fluorescent dye, biotin or an epitope tag. They selectively react with an enzyme target, resulting in its covalent labelling and attachment of the reporter, which can be detected and quantified. As GH99 enzymes lack an enzymatic nucleophile they cannot be labelled with any of a range of reagents that have been developed for this purpose such as 2-deoxyfluorosugars and cyclohexane epoxides and aziridines.[46] Overkleeft and co-workers noted that the glutamate residue that acts as a general base in the enzymatic mechanism might have potential as a labeling site. The two spiro epoxides were synthesized that place an electrophilic site near this glutamate, and were equipped with a fluorescent tag to allow visualization (Figure 6).[47] Upon incubation with recombinant enzyme, these reagents allowed concentration, time and pH dependent labelling of *Bt*GH99, and labelling could be competed by various substrates and inhibitors. These probes or related

Israel Journal of Chemistry

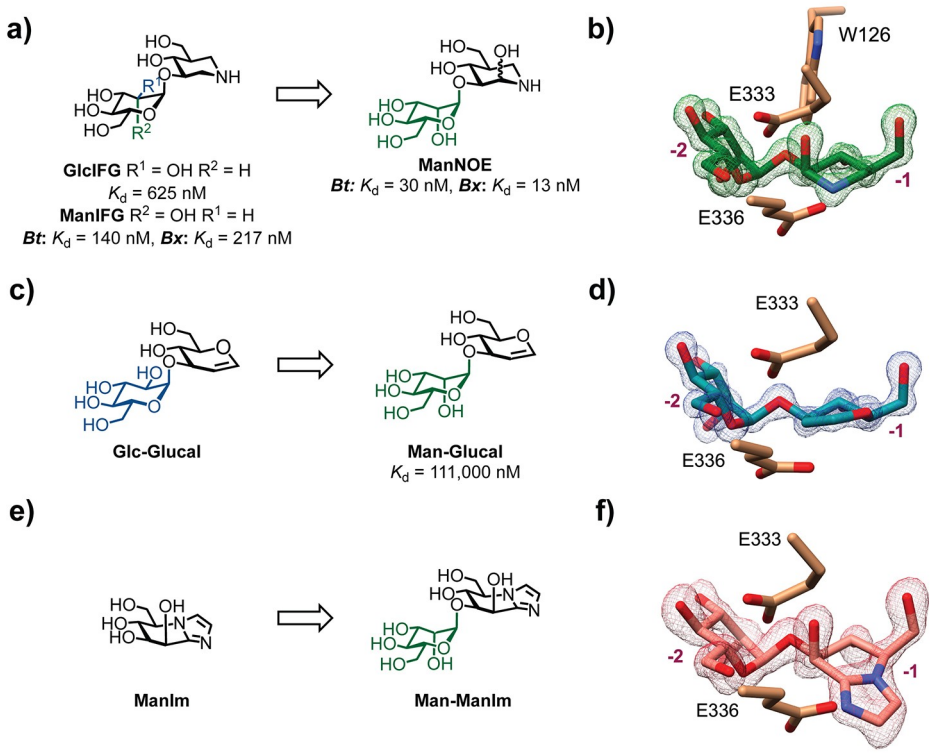

Figure 5. Strategies for inhibitor design for gut bacterial *endo*-α-1,2-mannanases. a) Variation of stereochemistry at the −2 sugar residue enhanced potency of GlcIFG to ManIFG, with further enhancement of activity by installation of the 2-OH group to give ManNOE. b) 3D X-ray structure of *Bx*GH99 bound to ManNOE (PDB 5LYR). The maximum-likelihood/σ_A-weighted $2F_{obs}–F_{calc}$ map is contoured at 0.77 $e^-/Å^{-3}$. c) Glc-Glucal is an inhibitor of MANEA, the corresponding Man-Glucal is an inhibitor of *Bx*GH99. d) 3D X-ray structure of *Bx*GH99 bound to Man-Glucal. (PDB 5 M5D). The maximum-likelihood/σ_A-weighted $2F_{obs}–F_{calc}$ map is contoured at 1.00 $e^-/Å^{-3}$. e) ManIm is a broad-spectrum inhibitor of exo-mannosidases; the corresponding Man-ManIm was prepared to target *endo*-α-1,2-mannanases. f) 3D X-ray structure of *Bx*GH99 bound to Man-ManIm. (PDB 6FAR). The maximum-likelihood/σ_A-weighted $2F_{obs}–F_{calc}$ map is contoured at 0.34 $e^-/Å^{-3}$.

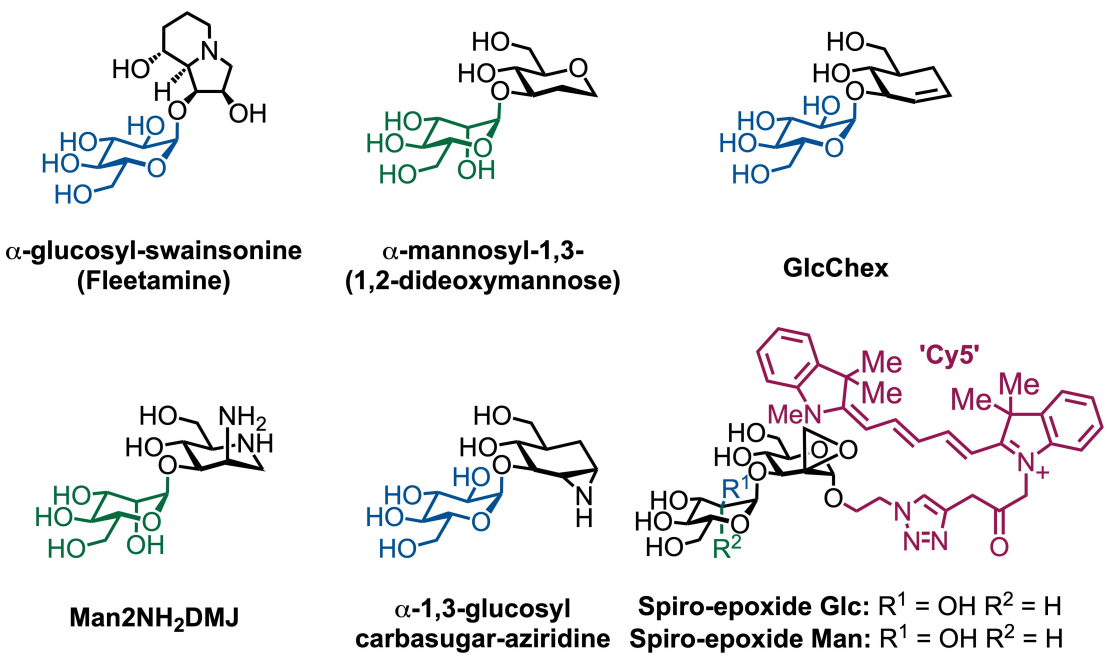

Figure 6. Structures of assorted inhibitor design concepts examined for inhibition of *endo*-α-1,2-mannosidase and *endo*-α-1,2-mannanase.

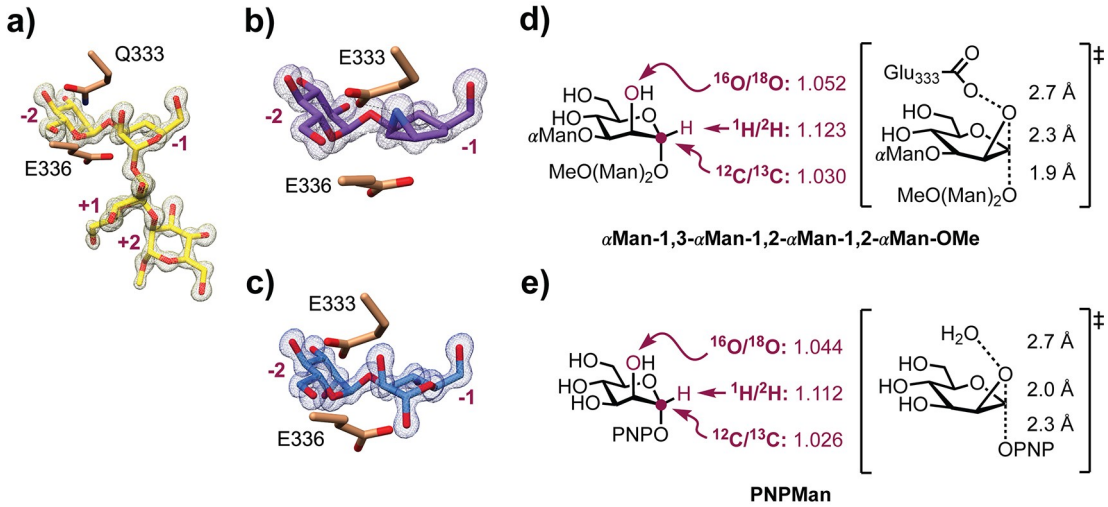

Figure 7. *Endo*-α-1,2-mannosidase proceeds through a mechanism involving a 1,2-anhydro sugar intermediate. a) 3D structure of 'Michaelis' complex of αMan-1,3-αMan-1,2-αMan-1,2-αMan-OMe (yellow) bound to *Bx*GH99-E333Q mutant (PDB 6FWG). b) Intermediate complex of cyclohexane β-1,2-aziridine (purple) with *Bx*GH99 (PDB 6FWI). c) product complex with α-1,3-mannobiose (blue, and α-1,2-mannobiose, not shown) with *Bx*GH99 (PDB 6FWP). The maximum-likelihood/σ_A-weighted $2F_{obs}–F_{calc}$ maps, shown in yellow, purple and blue, respectively, are contoured at 0.86, 0.61 and 0.91 $e^-/Å^3$, respectively. d) Summary of kinetic isotope effects measured at C1, H1 and O2 for the BtGH99 catalyzed hydrolysis of αMan-1,3-αMan-1,2-αMan-1,2-αMan-OMe. At right, calculated transition state structure. e) Summary of kinetic isotope effects of the hydroxide-promoted hydrolysis of *p*-nitrophenyl α-D-mannopyranoside. At right, calculated transition state structure.

derivatives may prove useful for functional investigation of GH99 enzymes in complex scenarios such as tissue extracts.

7. Structure and Mechanism of Human Endo-α-1,2-Mannosidase MANEA

Ito, Kajihara and colleagues reported the development of a system for heterologous expression of the catalytic domain of MANEA in *E. coli*, driven by a cold-induced promoter system in the presence of GroEL chaperones.[17] Using a similar approach we produced milligram quantities of a truncated MANEA protein, consisting of the catalytic domain beyond the stem domain (hereafter MANEA-Δ97).[48] MANEA-Δ97 was crystallized in the presence of Anderson-Evans polyoxotungstate $[TeW_6O_{24}]^{6-}$ (TEW) to give a form containing HEPES, which could be readily displaced by soaking with ligands. The 3D structure of MANEA-Δ97 is similar to those for *Bt*GH99 and *Bx*GH99 (with which MANEA shares 40% sequence identity) and with Cα rmsd >0.9 A over 333 matched residues (Figure 8a). One key difference was the presence of a flexible loop (residues 191–201), was found in various conformations in different crystal forms, and which could make interactions with the −2 Glc residue (Figure 8b). MANEA can process di- and tri-glucosylated N-glycans; possibly, this flexible loop provides a structural basis for this activity.

3D structures of complexes of wildtype MANEA-Δ97 with GlcIFG and α-1,2-mannobiose (Figure 8b), or of the E404Q mutant with the tetrasaccharide αGlc-1,3-αMan-1,2-αMan-1,2-αMan-OMe (Figure 8c), allowed detailed insight into the active site structure.[48] The catalytic residues around the reactive center are identical in location as for equivalent *Bx*GH99 complexes, suggesting a conserved mechanism with the bacterial GH99 members. This includes E407 that is proposed to act as general base in the formation of the 1,2-anhydro sugar intermediate, and E404 that acts as general acid to assist in departure of the anomeric leaving group. The substrates for MANEA and the bacterial GH99 members differ in the −2 sugar residues, which are Glc in the former and Man in the latter. As noted previously, the preference for Man over Glc in the bacterial enzymes arises from a hydrophobic interaction with C2 of this sugar residue. Within MANEA, the equivalent residue is Tyr189, which makes a water mediated hydrogen bonded interaction with the 2-OH of Glc in the complexes studied.

8. MANEA as an Antiviral Host Glycosylation Target

Enveloped viruses include coronaviruses, retroviruses, ebolaviruses, hepatitis B virus, influenza virus.[49] The envelope consists of portions of the host cell membrane that bud off from infected cells, and usually contains specific viral glycoproteins that are biosynthesized by coopting the host cell machinery during replication.[50–52] Inhibition of host glycosylation pathways have been shown to interfere with the viral

Israel Journal of Chemistry

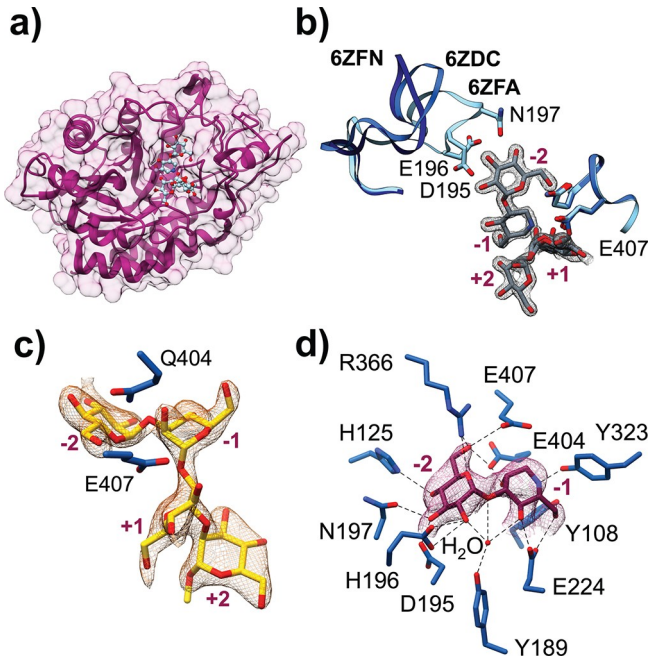

Figure 8. Structural insights into conformation and ligand binding of *H. sapiens* MANEA. a) 3D structure of MANEA-Δ97 in complex with GlcIFG and α-1,2-mannobiose (PDB 6ZFA). b) Superposition of different 3D structures highlighting the flexible loop of residues 191–201. MANEA-E404Q structure in complex with methyl α-1,2-mannobioside, ligand not shown (dark blue; PBD 6ZFN), MANEA + Ni^{2+} structure (mid-blue; PDB 6ZDC), and MANEA with GlcIFG and α-1,2 mannobiose structure (light blue; ligands: gray; PDB 6ZFA). The maximum-likelihood/σ_A-weighted $2F_{obs}–F_{calc}$ map, shown in grey, is contoured at 0.85, 0.50 and 0.78 $e^-/Å^3$, respectively. c) 3D structure of complex of MANEA–E404Q with αGlc-1,3-αMan-1,2-αMan-1,2-αMan-OMe. The maximum-likelihood/σ_A-weighted $2F_{obs}–F_{calc}$ map is contoured at 0.44 $e^-/Å^3$. d) Active site interactions between residues in MANEA, blue, and GlcDMJ, purple (PDB 6ZJ5). The maximum-likelihood/σ_A-weighted $2F_{obs}–F_{calc}$ map shown in purple is contoured at 0.43 $e^-/Å^3$ clipped to Glc and 0.27 e-/$Å^3$ clipped to DMJ.

lifecycle, impairing secretion, fusion or evasion of host immunity.[50,53] One fascinating example of the possible effect of targeting host glycosylation is provided by individuals with a congenital disorder of glycosylation (CDG) that lack glucosidase I (MOGS). Anecdotally, these individuals exhibit resistance to viral infections,[54] which presumably relate to dysfunction of viral particle assembly or infectivity upon alteration of their normal N-linked glycans. While most efforts to target host glycosylation processes have focused on the classical glucosidase dependent N-linked glycosylation pathway, it has been shown that in the case of hepatitis B virus that when glucosidases are inhibited, mature viral glycoproteins are still produced through the endomannosidase pathway.[55] Nonetheless, even a partial knockdown of N-glycosylation machinery appears to be sufficient to alter the course of viral infection as shown in the case of MOGS-CDG individuals, which still maintain functional endomannosidase pathway. Likewise, it is possible that drugs targeting the endomannosidase pathway could reduce viral viability, even in the presence of the glucosidase pathway.

Karaivanova *et al.* showed that treatment of cells infected with vesicular stomatis virus with GlcDMJ led to changes in the structure of the N-glycan on the VSV G glycoprotein, as shown by their change in susceptibility to digestion by endo H (*endo*-β-*N*-acetylglucosaminidase).[56] Likewise, we showed that treatment of MDBK cells infected with bovine viral diarrhea virus with GlcIFG resulted in increased sensitivity of envelope glycoproteins to endo H digestion, which mirrors that induced by treatment with NAP-DNJ, an inhibitor of glucosidase I/II (Figure 9).[48] Co-treatment with NAP-DNJ and GlcIFG gave even greater sensitivity to endo H. Reinfection assays showed a reduction in number of infected cells, with additive effects from co-treatment with NAP-DNJ and GlcIFG, suggesting that the change in N-glycan structure alters infectivity.

Dengue virus is transmitted by mosquito and causes a flu-like illness that usually resolves but can be more serious and even lead to death. It is an enveloped virus that contains two glycoproteins: envelope (E) and non-structural protein 1 (NS1).[57] Treatment of infected Huh7.5 cells with GlcIFG or GlcDMJ did not affect viral particle formation, as assessed by levels of secreted viral RNA. However, reinfection assays showed that both compounds reduced DENV reinfectivity, with a six-fold reduction for GlcDMJ at 1 mM.[48]

9. Conclusions and Summary

Family GH99 is now known to contain two main activities, *endo*-α-1,2-mannosidase and *endo*-α-1,2-mannanase. As the key enzyme of the *endo*-α-1,2-mannosidase pathway, MANEA provides a glucosidase independent pathway for N-glycan maturation. Because of its critical role in N-glycan maturation, it is a promising target for host directed antiviral intervention. Structure guided synthesis of inhibitors have led to the development of potent inhibitors of MANEA with antiviral activity against enveloped viruses, providing proof of concept of a novel host-directed antiviral approach. While GH99 enzymes from gut *Bacteroides* spp. also possess *endo*-α-1,2-mannosidase activity, their specific expression under conditions of growth on yeast mannan as well as their preference for mannose-configured substrates leads to their assignment as *endo*-α-1,2-mannanases. This activity allows the processing of hypermannosylated sidechains on yeast N-glycans in the human gut as part of the complex catabolic pathway that allows utilization of yeast α-mannan as a nutrient. In addition to their importance in processing of mammalian and fungal N-linked glycans, enzymes of family GH99 have significant potential in chemoenzymatic synthesis as transglycosylation catalysts[58] and through 'top down' trimming approaches to high mannose N-linked glycans.[59] Uniquely, the available evidence suggests that both classes of enzymes utilize a

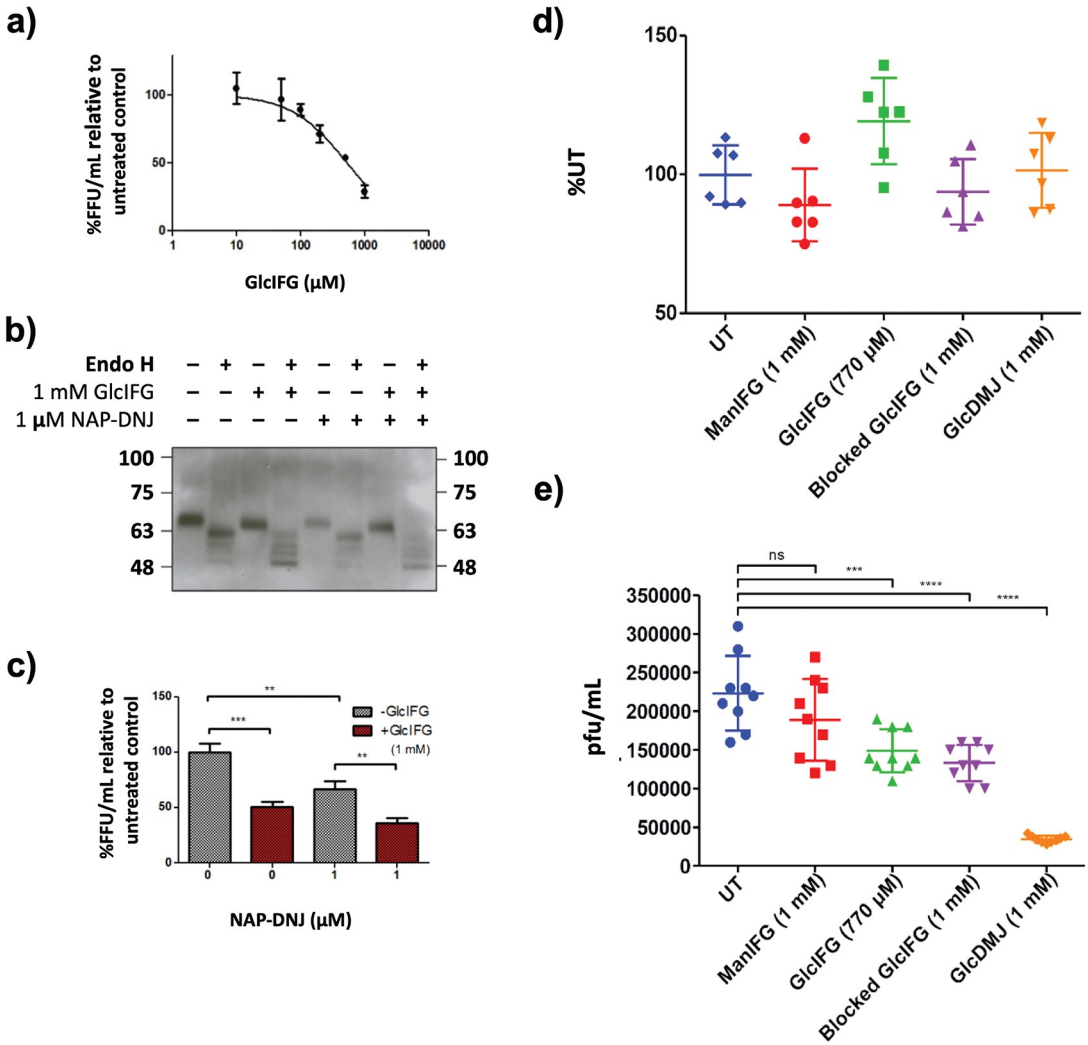

Figure 9. Antiviral action of MANEA inhibitors. Results of BVDV reinfection assays in MDBK cells, (a–c) and DENV reinfection assays in Huh7.5 cells (d and e). (a) Percentage of focus forming using (FFU)/mL relative to untreated cells at different concentrations of GlcIFG, at a multiplicity of infection of 1. (b) Effect of MANEA inhibition (GlcIFG) and ER glucosidase II inhibition (NAP-DNJ) on the susceptibility of glycans on the BVDV E1/E2 protein to cleavage by endo H. (c) The combined effects of NAP-DNJ and GlcIFG on BVDV infectivity, as measured by FFU/mL. Experiments were performed in triplicate. (d) Secreted RNA levels in DENV-infected Huh7.5 cells. (e) Reinfectivity plaque assay from DENV-infected Huh7.5 cells. The horizontal bar in (d) and (e) indicates the mean. This figure is reproduced from ref.[61] under the Creative Commons Attribution-NonCommercial-NoDerivatives License 4.0 (CC BY-NC-ND), https://creativecommons.org/licenses/by-nc-nd/4.0/.

catalytic mechanism involving a 1,2-anhydro sugar intermediate.

Acknowledgements

We thank the Australian Research Council (DP210100233; DP210100235). GJD thanks the Royal Society for a Ken Murray Research Professorship. Open Access publishing facilitated by The University of Melbourne, as part of the Wiley - The University of Melbourne agreement via the Council of Australian University Librarians.

Data Availability Statement

The data that support the findings of this study are available from the corresponding author upon reasonable request.

References

[1] J. J. Caramelo, A. J. Parodi, *FEBS Lett.* **2015**, *589*, 3379–3387.
[2] R. Apweiler, H. Hermjakob, N. Sharon, *Biochim. Biophys. Acta* **1999**, *1473*, 4–8.

[3] R. Kornfeld, S. Kornfeld, *Annu. Rev. Biochem.* **1985**, *54*, 631–664.
[4] A. Helenius, M. Aebi, *Annu. Rev. Biochem.* **2004**, *73*, 1019–1049.
[5] A. Varki, *Glycobiology* **2017**, *27*, 3–49.
[6] C. Reily, T. J. Stewart, M. B. Renfrow, J. Novak, *Nat. Rev. Nephrol.* **2019**, *15*, 346–366.
[7] M. Aebi, *Biochim. Biophys. Acta* **2013**, *1833*, 2430–2437.
[8] P. Burda, M. Aebi, *Biochim. Biophys. Acta* **1999**, *1426*, 239–257.
[9] T. Kuribara, K. Totani, *Curr. Opin. Struct. Biol.* **2021**, *68*, 41–47.
[10] T. Kuribara, M. Hirano, G. Speciale, S. J. Williams, Y. Ito, K. Totani, *Chembiochem : a European journal of chemical biology* **2017**, *18*, 1027–1035.
[11] S. S. Vembar, J. L. Brodsky, *Nat. Rev. Mol. Cell Biol.* **2008**, *9*, 944–957.
[12] J. Lombard, *Biol. Direct.* **2016**, *11*, 36.
[13] J. Roth, M. Ziak, C. Zuber, *Biochimie* **2003**, *85*, 287–294.
[14] K. Dairaku, R. G. Spiro, *Glycobiology* **1997**, *7*, 579–586.
[15] W. A. Lubas, R. G. Spiro, *J. Biol. Chem.* **1988**, *263*, 3990–3998.
[16] S. E. Moore, R. G. Spiro, *J. Biol. Chem.* **1992**, *267*, 8443–8451.
[17] S. Dedola, M. Izumi, Y. Makimura, A. Seko, A. Kanamori, Y. Takeda, Y. Ito, Y. Kajihara, *Carbohydr. Res.* **2016**, *434*, 94–98.
[18] C. M. De Praeter, G. J. Gerwig, E. Bause, L. K. Nuytinck, J. F. Vliegenthart, W. Breuer, J. P. Kamerling, M. F. Espeel, J. J. Martin, A. M. De Paepe, N. W. Chan, G. A. Dacremont, R. N. Van Coster, *Am. J. Hum. Genet.* **2000**, *66*, 1744–1756.
[19] S. Weng, R. G. Spiro, *Glycobiology* **1996**, *6*, 861–868.
[20] S. E. Moore, R. G. Spiro, *J. Biol. Chem.* **1990**, *265*, 13104–13112.
[21] W. A. Lubas, R. G. Spiro, *J. Biol. Chem.* **1987**, *262*, 3775–3781.
[22] E. Drula, M.-L. Garron, S. Dogan, V. Lombard, B. Henrissat, N. Terrapon, *Nucleic Acids Res.* **2021**, *50*, D571–D577.
[23] *Glycobiology* **2018**, *28*, 3–8.
[24] M. J. Spiro, V. D. Bhoyroo, R. G. Spiro, *J. Biol. Chem.* **1997**, *272*, 29356–29363.
[25] A. J. Thompson, R. J. Williams, Z. Hakki, D. S. Alonzi, T. Wennekes, T. M. Gloster, K. Songsrirote, J. E. Thomas-Oates, T. M. Wrodnigg, J. Spreitz, A. E. Stutz, T. D. Butters, S. J. Williams, G. J. Davies, *Proc. Natl. Acad. Sci. USA* **2012**, *109*, 781–786.
[26] K. Matsuda, Y. Kurakata, T. Miyazaki, I. Matsuo, Y. Ito, A. Nishikawa, T. Tonozuka, *Biosci. Biotechnol. Biochem.* **2011**, *75*, 797–799.
[27] U. Spohr, M. Bach, R. G. Spiro, *Can. J. Chem.* **1993**, *71*, 1928–1942.
[28] S. Hiraizumi, U. Spohr, R. G. Spiro, *J. Biol. Chem.* **1993**, *268*, 9927–9935.
[29] C. Rovira, A. Males, G. J. Davies, S. J. Williams, *Curr. Opin. Struct. Biol.* **2020**, *62*, 79–92.
[30] M. Brockhaus, H.-M. Dettinger, G. Kurz, J. Lehmann, K. Wallenfels, *Carbohydr. Res.* **1979**, *69*, 264–268.
[31] K. Wallenfels, R. Weil, in: *The Enzymes, Vol. 7*, 3rd Edition ed. (Ed.: P. D. Boxer), Academic Press, New York, **1972**, pp. 617–663.
[32] J. C. Gebler, R. Aebersold, S. G. Withers, *J. Biol. Chem.* **1992**, *267*, 11126–11130.
[33] F. Cuskin, E. C. Lowe, M. J. Temple, Y. Zhu, E. A. Cameron, N. A. Pudlo, N. T. Porter, K. Urs, A. J. Thompson, A. Cartmell, A. Rogowski, B. S. Hamilton, R. Chen, T. J. Tolbert, K. Piens, D. Bracke, W. Vervecken, Z. Hakki, G. Speciale, J. L. Munoz-Munoz, A. Day, M. J. Pena, R. McLean, M. D. Suits, A. B. Boraston, T. Atherly, C. J. Ziemer, S. J. Williams, G. J. Davies, D. W. Abbott, E. C. Martens, H. J. Gilbert, *Nature* **2015**, *517*, 165–169.
[34] Z. Hakki, A. J. Thompson, S. Bellmaine, G. Speciale, G. J. Davies, S. J. Williams, *Chem. Eur. J.* **2015**, *21*, 1966–1977.
[35] H. J. Atkinson, J. H. Morris, T. E. Ferrin, P. C. Babbitt, *PLoS One* **2009**, *4*, e4345.
[36] H. Liu, X. Liang, H. Søhoel, A. Bülow, M. Bols, *J. Am. Chem. Soc.* **2001**, *123*, 5116–5117.
[37] M. Petricevic, L. F. Sobala, P. Fernandes, L. Raich, A. J. Thompson, G. Bernardo-Seisdedos, O. Millet, S. Zhu, M. Sollogoub, J. Jimenez-Barbero, C. Rovira, G. J. Davies, S. J. Williams, *J. Am. Chem. Soc.* **2017**, *139*, 1089–1097.
[38] P. Z. Fernandes, M. Petricevic, L. Sobala, G. J. Davies, S. J. Williams, *Chem. Eur. J.* **2018**, *24*, 7464–7473.
[39] T. Quach, S. Tsegay, A. J. Thompson, N. V. Kukushkin, D. S. Alonzi, T. D. Butters, G. J. Davies, S. J. Williams, *Tetrahedron: Asymmetry* **2012**, *23*, 992–997.
[40] D. Lu, S. Zhu, L. F. Sobala, G. Bernardo-Seisdedos, O. Millet, Y. Zhang, J. Jimenez-Barbero, G. J. Davies, M. Sollogoub, *Org. Lett.* **2018**, *20*, 7488–7492.
[41] L. F. Sobala, G. Speciale, S. Zhu, L. Raich, N. Sannikova, A. J. Thompson, Z. Hakki, D. Lu, S. Shamsi Kazem Abadi, A. R. Lewis, V. Rojas-Cervellera, G. Bernardo-Seisdedos, Y. Zhang, O. Millet, J. Jiménez-Barbero, A. J. Bennet, M. Sollogoub, C. Rovira, G. J. Davies, S. J. Williams, *ACS Cent. Sci.* **2020**, *6*, 760–770.
[42] D. J. Vocadlo, *ACS Cent. Sci.* **2020**, *6*, 619–621.
[43] G. Speciale, M. Farren-Dai, F. S. Shidmoossavee, S. J. Williams, A. J. Bennet, *J. Am. Chem. Soc.* **2016**, *138*, 14012–14019.
[44] R. C. Gasman, D. C. Johnson, *J. Org. Chem.* **1966**, *31*, 1830–1838.
[45] J. Chan, A. R. Lewis, M. Gilbert, M. F. Karwaski, A. J. Bennet, *Nat. Chem. Biol.* **2010**, *6*, 405–407.
[46] L. Wu, Z. Armstrong, S. P. Schroder, C. de Boer, M. Artola, J. M. Aerts, H. S. Overkleeft, G. J. Davies, *Curr. Opin. Chem. Biol.* **2019**, *53*, 25–36.
[47] S. P. Schroder, W. W. Kallemeijn, M. F. Debets, T. Hansen, L. F. Sobala, Z. Hakki, S. J. Williams, T. J. M. Beenakker, J. Aerts, G. A. van der Marel, J. D. C. Codee, G. J. Davies, H. S. Overkleeft, *Chem. Eur. J.* **2018**, *24*, 9983–9992.
[48] F. Sobala Ł, P. Z. Fernandes, Z. Hakki, A. J. Thompson, J. D. Howe, M. Hill, N. Zitzmann, S. Davies, Z. Stamataki, T. D. Butters, D. S. Alonzi, S. J. Williams, G. J. Davies, *Proc. Natl. Acad. Sci. USA* **2020**, *117*, 29595–29601.
[49] F. A. Rey, S.-M. Lok, *Cell* **2018**, *172*, 1319–1334.
[50] I. Bagdonaite, H. H. Wandall, *Glycobiology* **2018**, *28*, 443–467.
[51] D. J. Vigerust, V. L. Shepherd, *Trends Microbiol.* **2007**, *15*, 211–218.
[52] Y. Li, D. Liu, Y. Wang, W. Su, G. Liu, W. Dong, *Front. Immunol.* **2021**, *12*, 638573.
[53] R. A. Dwek, J. I. Bell, M. Feldmann, N. Zitzmann, *Lancet* **2022**, *399*, 1381–1382.
[54] M. A. Sadat, S. Moir, T. W. Chun, P. Lusso, G. Kaplan, L. Wolfe, M. J. Memoli, M. He, H. Vega, L. J. Y. Kim, Y. Huang, N. Hussein, E. Nievas, R. Mitchell, M. Garofalo, A. Louie, D. C. Ireland, C. Grunes, R. Cimbro, V. Patel, G. Holzapfel, D. Salahuddin, T. Bristol, D. Adams, B. E. Marciano, M. Hegde, Y. Li, K. R. Calvo, J. Stoddard, J. S. Justement, J. Jacques, D. A. L. Priel, D. Murray, P. Sun, D. B. Kuhns, C. F. Boerkoel, J. A. Chiorini, G. Di Pasquale, D. Verthelyi, S. D. Rosenzweig, *N. Engl. J. Med.* **2014**, *370*, 1615–1625.
[55] A. Mehta, X. Lu, T. M. Block, B. S. Blumberg, R. A. Dwek, *Proc. Natl. Acad. Sci. USA* **1997**, *94*, 1822–1827.
[56] V. K. Karaivanova, P. Luan, R. G. Spiro, *Glycobiology* **1998**, *8*, 725–730.
[57] D. L. Carbaugh, H. M. Lazear, *J. Virol.* **2020**, *94*.

[58] S. Iwamoto, Y. Kasahara, Y. Yoshimura, A. Seko, Y. Takeda, Y. Ito, K. Totani, I. Matsuo, *Chembiochem : a European journal of chemical biology* **2017**, *18*, 1376–1378.
[59] A. Koizumi, I. Matsuo, M. Takatani, A. Seko, M. Hachisu, Y. Takeda, Y. Ito, *Angew. Chem. Int. Ed.* **2013**, *52*, 7426–7431; *Angew. Chem.* **2013**, *125*, 7574–7579.
[60] R. Zallot, N. Oberg, J. A. Gerlt, *Biochemistry* **2019**, *58*, 4169–4182.
[61] L. F. Sobala, P. Fernandes, Z. Hakki, A. J. Thompson, J. Howe, M. Hill, N. Zitzmann, S. Davies, Z. Stamataki, T. D. Butters, D. S. Alonzi, S. J. Williams, G. J. Davies, *Proc. Natl. Acad. Sci. USA* **2020**, *117*, 29595–29601.

Manuscript received: August 30, 2022
Revised manuscript received: September 19, 2022
Version of record online: October 19, 2022